High-Pressure Elastic Properties of Solid Argon to 70 GPa

Hiroyasu Shimizu, Hideyuki Tashiro, Tetsuji Kume, and Shigeo Sasaki

Department of Electronics, Gifu University, 1-1 Yanagido, Gifu 501-1193, Japan
and CREST, Japan Science and Technology Corporation (JST), Kawaguchi, Saitama 332-0012, Japan

(Received 6 December 2000)

The acoustic velocities, adiabatic elastic constants, bulk modulus, elastic anisotropy, Cauchy violation, and density in an ideal solid argon (Ar) have been determined at high pressures up to 70 GPa in a diamond anvil cell by making new approaches of Brillouin spectroscopy. These results place the first complete study for elastic properties of dense Ar and provide an improved basis for making the theoretical calculations of rare-gas solids over a wide range of compression.

DOI: 10.1103/PhysRevLett.86.4568 PACS numbers: 62.50.+p, 62.65.+k, 64.70.Kb, 78.35.+c

The rare-gas argon (Ar) is the third component of dry air in its volume, and is among the simplest in nature because of its closed-shell electronic configuration. Rare-gas van der Waals solids are an important class of materials [1,2] to provide an ideal system allowing fruitful comparisons between experiments and theoretical calculations [1]. A considerable amount of effort has been expended in attempts to determine the interatomic potentials for rare-gas solids, including possible effects of many-body forces [1,3,4]. The elastic properties of dense Ar are of fundamental interest as the hydrostatic pressure medium for high-pressure research in a diamond anvil cell (DAC) and as a component in rocks and the atmospheres of planetary bodies.

At ambient pressure, Ar liquefies at 87.3 K and solidifies in the fcc phase at 83.8 K. At 300 K, the liquid Ar crystallizes into the same phase at about $P = 1.3$ GPa [5,6]. With increasing pressure, a single crystal Ar grown in the DAC always recrystallizes to a small group of single crystals at a pressure of about 4 GPa [5,7]. This crystalline behavior of solid Ar needs careful experiments above $P = 4$ GPa in order to obtain the reliable elastic properties, because the acoustic velocities are sensitive to the crystal direction [8–10].

Gewurtz and Stoicheff measured the Brillouin scattering of the fcc crystalline Ar at 82.3 K and 1 atm, and determined three adiabatic elastic constants [11]. Grimsditch *et al.* [7] determined the pressure dependence of three elastic constants up to 33 GPa at 300 K by Brillouin spectroscopy. They measured only the longitudinal acoustic (LA) mode of solid Ar in a DAC using a backscattering geometry without identification of the crystal orientations, and estimated the envelope curves which correspond to the maximum and the minimum LA velocities for all measured points. (Hereafter, we designate this type of max and min method as the envelope method.)

Here we present the pressure dependences of acoustic velocities, adiabatic elastic constants, bulk modulus, elastic anisotropy, Cauchy violation, and density of the solid Ar at pressures up to 70 GPa, which were determined by making new approaches that combine the method of *in situ* Brillouin spectroscopy [9] for a single crystal Ar up to 4 GPa and the envelope method applied to both LA and transverse acoustic (TA) modes for the recrystallized Ar between 4 and 70 GPa. These results with greater certainty are compared with the earlier study [7] up to 33 GPa, and provide an improved basis for investigating elastic properties of dense Ar and give testing grounds for theories of lattice dynamics and interatomic potentials over a wide range of compression.

Experimental and analysis.—For loading an Ar sample in the DAC, we pressurized commercial gaseous Ar above $P_c = 48.1$ atm in a high-pressure gas vessel, including the DAC with an empty gasket hole, and sealed its fluid Ar in the sample chamber of the DAC. A single crystal of Ar was grown by increasing the pressure on a seed crystal, which coexists with the liquid Ar at $P = 1.3$ GPa and 300 K. The structure of the crystalline Ar is the fcc, but it does not show the crystal habit in the DAC. No pressure transmitting medium was used, because solid Ar is a soft material. The pressure was measured by the ruby-scale method [12]. Solid Ar becomes nonhydrostatic around 10 GPa [13,14], but it still provides a quasihydrostatic environment at very high pressures [15]. To minimize the effect of the pressure gradients in the Ar sample across the anvil, we used a tightly focused laser spot less than 10 μm, which is smaller than the sample size (about 50 μm). The 514.5 nm argon-ion laser line (λ_0) with a single longitudinal mode was used at an input power of about 100 mW. The heart of the apparatus was a Sandercock tandem Fabry-Perot interferometer [16], which was used in a triple-pass arrangement. The Brillouin frequency shift ($\Delta\nu$) at 60° scattering geometry with the DAC is related to the acoustic velocity (v) as follows [8]: $\Delta\nu_{60} = v_{60}/\lambda_0$. For the single crystal Ar at low pressures between 1.3 and 4 GPa, the elastic properties have been studied by using the method of *in situ* Brillouin spectroscopy developed for simple molecular solids [9,10]. The Brillouin frequency shift ($\Delta\nu$) can be calculated theoretically by using the above relation between $\Delta\nu$ and v, and the solution of the elastic equation as follows [9,10]: $v_j = f_j(C_{11}/\rho, C_{12}/\rho, C_{44}/\rho, \theta, \phi, \chi)$, where the subscript j ($= 0, 1, 2$) indicates LA, TA_1 (slow), and TA_2 (fast) modes, respectively, and C_{ij} the adiabatic elastic constant, ρ the density, and the Euler angles (θ, ϕ, χ) indicate the crystal orientation in the DAC.

 0031-9007/01/86(20)/4568(4)$15.00

For the recrystallized Ar at high pressures between 4 and 70 GPa, we applied the envelope method to both LA and TA modes; the maximum and the minimum values of acoustic velocities are estimated by measuring the direction dependence of acoustic velocities at each pressure, and by using these distributed velocity data we can determine the envelope curves for LA and TA modes. Then, the relations can be derived from theoretical predictions that the maximum LA velocity exists along the ⟨111⟩ directions and is represented by $v_{\mathrm{LA,max}} = [(C_{11} + 2C_{12} + 4C_{44})/(3\rho)]^{1/2}$, and the minimum LA velocity along the ⟨100⟩ directions; $v_{\mathrm{LA,min}} = (C_{11}/\rho)^{1/2}$, and the maximum TA velocity along the ⟨100⟩ directions; $v_{\mathrm{TA,max}} = (C_{44}/\rho)^{1/2}$, and the minimum TA velocity along the ⟨110⟩ direction; $v_{\mathrm{TA,min}} = [(C_{11} - C_{12})/(2\rho)]^{1/2}$.

Results and discussion.—For the single crystal Ar at low pressures between 1.3 and 4 GPa, we could observe clearly one LA and two TA modes on the Brillouin spectra. By rotating the DAC at about 10° intervals along the load axis, we measured the ϕ dependence of Brillouin frequency shifts (i.e., acoustic velocities) at each pressure. The computerized least-squares fit was applied to determine three elastic constants and Euler angles [9,10]. We could get the best fitting to the measured values at each pressure, which yielded, for example, $C_{11}/\rho = 10.2$, $C_{12}/\rho = 7.48$, and $C_{44}/\rho = 4.17$ km^2/s^2 at $P = 3.48$ GPa. Once the six parameters were determined, the acoustic velocities could be calculated for all directions. In Fig. 1 and its inset, the squares of sound velocities corresponding to $v_{\mathrm{LA,max}}$, $v_{\mathrm{LA,min}}$, $v_{\mathrm{TA,max}}$, and $v_{\mathrm{TA,min}}$ are plotted by solid symbols up to 4 GPa at 300 K. Next, we estimated the pressure dependence of the ratio of specific heats, $\gamma = C_P/C_V = B_S/B_T$, where the adiabatic bulk modulus B_S [$= (C_{11} + 2C_{12})/3$] is determined from the present Brillouin results and the isothermal bulk modulus B_T [$= \rho(dP/d\rho)_T$] from x-ray studies [5,17]. The value of γ shows 1.21 at $P = 1.5$ GPa and decreases to 1.08 at 4 GPa with increasing pressure. By using 15 data points between 1.3 and 4 GPa and taking account of its expected pressure behavior [18], we obtained the fitted curve of $\gamma(P) = 1 + 0.383\exp(-0.389P)$, which shows almost $\gamma = 1$ at pressures above 20 GPa. These behaviors are reasonable for the simple molecular solids [19,20]. We calculated the ρ by the use of the following equation [8]:

$$\rho(P) = \rho(P_r) + \int_{P_r}^{P} (\gamma/V_B^2)\, dP\,, \qquad (1)$$

where $P_r = 1.3$ GPa and $\rho(P_r) = 2.02$ g/cm^3 [5,17], and the bulk sound velocity is represented as $V_B = [(C_{11} + 2C_{12})/(3\rho)]^{1/2}$. Our calculated results of $\rho(P)$ and the densities determined by x-ray studies [5,17] are shown in Fig. 2 by a solid line and open circles, respectively. Their agreement is excellent at these pressures.

Next, by the use of the equation of state obtained above, we determined elastic constants C_{11}, C_{12}, and C_{44} up to 4 GPa, which are plotted by solid symbols up to 4 GPa in the inset of Fig. 3. They increase almost linearly with increasing pressure. For the comparison with the earlier Brillouin study, we also show their experimental results [7] by open symbols. The notable discrepancy can be found on the values of C_{11} and C_{12}, which are due to the earlier measurements of only LA velocity for unknown directions of an Ar single crystal.

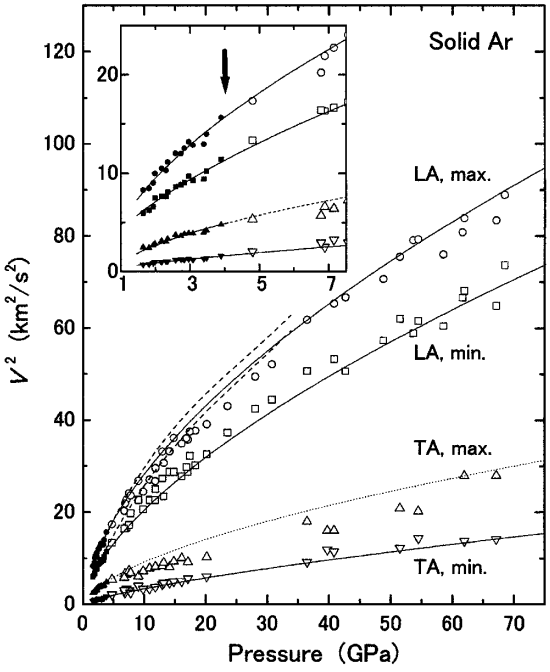

FIG. 1. Pressure dependence of the squares of $v_{\mathrm{LA,max}}$, $v_{\mathrm{LA,min}}$, $v_{\mathrm{TA,max}}$, and $v_{\mathrm{TA,min}}$. Solid symbols below $P = 4$ GPa (see the inset) indicate experimental points determined directly by the *in situ* Brillouin method. Vertical arrow indicates the Ar recrystallization point at $P = 4$ GPa. Three solid lines show the envelope curves of maximum and minimum velocities of solid Ar up to $P = 70$ GPa, and one dashed line shows the envelope curve estimated from above three envelope curves. The two broken lines show the earlier data [7] of envelope curves for the LA mode up to 33 GPa.

At pressures above 4 GPa, the probed single crystals in the recrystallized Ar are randomly oriented and, as a result, we should observe the spread of the experimental points of acoustic velocities. We estimated the maximum and the minimum velocities of observed LA and TA modes in many different runs by measuring the direction dependence of acoustic velocities at each pressure. In Fig. 1, experimental results are plotted by open symbols for LA and TA modes up to 70 GPa. We determined the envelope curves for LA and TA modes self-consistently by extrapolating the reliable low-pressure data and by interpolating the high-pressure data around $P = 4$ GPa. Since the Brillouin signal for the maximum velocity of the TA_2 mode corresponding to $(C_{44}/\rho)^{1/2}$ was hardly observed, the value of $v_{\mathrm{TA,max}}$ could not be precisely estimated. However, it is enough to determine three elastic constants by using three relations for $v_{\mathrm{LA,max}}$, $v_{\mathrm{LA,min}}$, and $v_{\mathrm{TA,min}}$. The obtained results can determine the value of $v_{\mathrm{TA,max}} = (C_{44}/\rho)^{1/2}$, and the squares of their velocities are reasonably represented by the dashed line in Fig. 1. The pressure

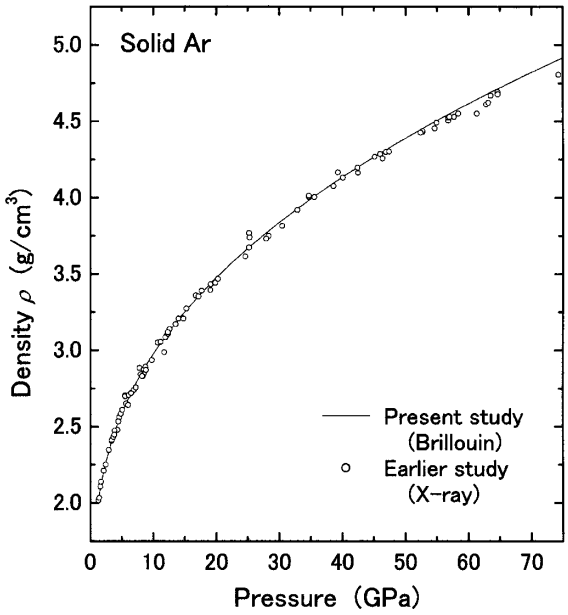

FIG. 2. Comparison of ρ-P equations of state for solid Ar. The solid curve is the equation of state determined by the present study using the Brillouin method. Also shown are earlier data points of the equation of state (open circles) from x-ray studies [5,17].

dependence of these estimated C_{11}/ρ, C_{12}/ρ, and C_{44}/ρ reveal the acoustic velocities for all directions of solid Ar up to 70 GPa. To compare with the earlier study [7] up to 33 GPa, we show Grimsditch *et al.*'s envelope curves for the LA mode by two broken lines in Fig. 1, which were calculated from their data of elastic moduli in Ref. [7] [Fig. 5 (below)]. The agreement for the square of $v_{\mathrm{LA,max}}$ is fairly good, but the disagreement for the square of $v_{\mathrm{LA,min}}$ is remarkable.

Next, we determined the equation of state of solid Ar between 4 and 70 GPa by the use of Eq. (1) with $\gamma(P)$ and V_B, and show the results in comparison with x-ray data [5,17] in Fig. 2. Their agreement is very good, which indicates our envelope method is self-consistent and is nicely applied. The present results of $\rho(P)$ yielded the determination of C_{11}, C_{12}, and C_{44} (B_S) as shown in Fig. 3. They increase monotonically with increasing pressure, and indicate $C_{11} = 340$, $C_{12} = 199$, and $C_{44} = 145$ GPa ($B_S = 246$ GPa) at $P = 70$ GPa. It is surprising that at pressures above 43 GPa the B_S of rare-gas solid Ar show larger values than that of bcc iron ($\sim$160 GPa) at 1 atm and 300 K [21]. There is no evidence of structural phase transformation over a wide range of pressure to 70 GPa, and the Born's stability conditions [18,22] are satisfied.

For the comparison with the earlier Brillouin study to 33 GPa, we also show their experimental results by open symbols [7] and their theoretical calculations by open symbols with a cross [7] in Fig. 3. The remarkable discrepancy can be found on C_{11} and C_{12}, which are due to the earlier study of (i) the uncertainty of the envelope curves determined by the use of only the LA mode based on the measurement of $n\upsilon$ at the backscattering geometry and (ii) the assumption of $B_S/B_T = \gamma = 1$ at all pressures. The theoretical calculations up to $P = 51$ GPa [7] remain

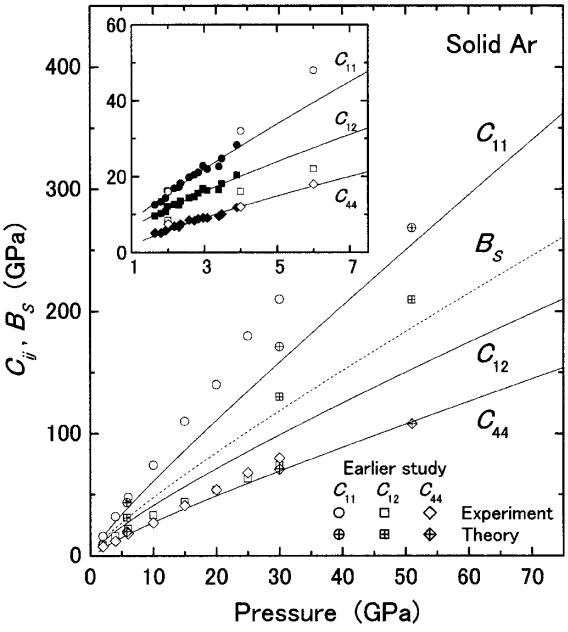

FIG. 3. Pressure dependence of three adiabatic elastic constants and adiabatic bulk modulus (B_S) for solid Ar up to 70 GPa at 300 K: present studies; solid lines (C_{11}, C_{12}, and C_{44}) and dashed line (B_S), earlier experiments to 33 GPa [7]; open symbols, theoretical calculations to 51 GPa [7]; open symbols with cross. The solid symbols in the inset show the present results of the *in situ* Brillouin method between 1.3 and 4 GPa.

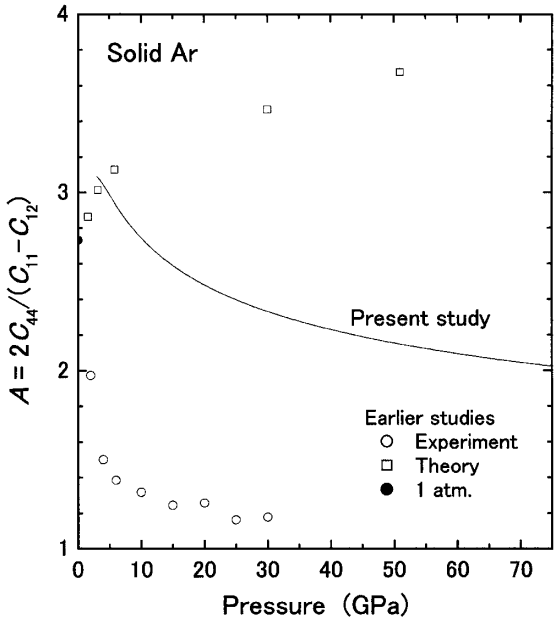

FIG. 4. Pressure dependence of the elastic anisotropy [$A = 2C_{44}/(C_{11} - C_{12})$] for solid Ar. The present result is shown by the solid line, and the earlier experimental and theoretical studies [7] are indicated by open circles and open squares, respectively. The solid circle shows the A value of low temperature solid Ar at atmospheric pressure [11].

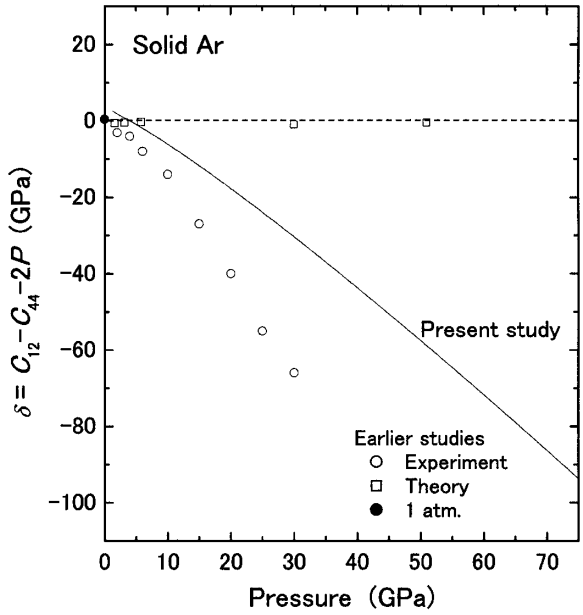

FIG. 5. Pressure dependence of the deviation from the Cauchy relation [δ ($= C_{12} - C_{44} - 2P$)] for solid Ar. The present result is shown by the solid line, and the earlier experimental and theoretical studies [7] are indicated by open circles and open squares, respectively. The solid circle shows the δ value ($= 0.44$ GPa) of low temperature solid Ar at atmospheric pressure [11].

discrepant with the present experimental results; they performed self-consistent phonon calculations using a pair potential proposed by Aziz and Chen [23].

A measure of the anisotropy of the elasticity is given by $A = 2C_{44}/(C_{11} - C_{12})$ for cubic crystals [9]. For isotropic elasticity, the two shear moduli C_{44} and $(C_{11} - C_{12})/2$ are equal and $A = 1$. The pressure dependence of this A for solid Ar was determined up to 70 GPa as shown in Fig. 4 (solid line), and compared with the earlier studies [7], including the low-temperature solid Ar at 1 atm [11]. The present result exhibits $A = 3.04$ at $P = 4$ GPa, and shows a gradual decrease to 2.05 at 70 GPa, which is reasonable, and this trend seems to be characteristic of the rare-gas solids [24].

The high-pressure Cauchy relation for hydrostatic conditions [7,25,26], $C_{12} = C_{44} + 2P$, is satisfied when interatomic forces are purely central. The deviations δ ($= C_{12} - C_{44} - 2P$) are caused by the effects due to many-body forces in a solid. Figure 5 shows the pressure dependence of our δ (solid line) and the earlier experiment and theoretical calculations (open symbols) [7] for solid Ar. One can see that their behaviors are remarkably different. The magnitude of the present experimental δ shows 2.59 GPa at $P = 1.3$ GPa, and decreases (greater Cauchy violation) to $\delta = -86.3$ GPa at $P = 70$ GPa with increasing pressure. This notable result of the Cauchy violation shows that the noncentral nature of the bonding becomes greater at higher pressures, which indicates an important role of many-body forces [3,4] in order to construct the best potentials of high-density solid Ar.

In conclusion, the present study has provided the first complete results for elastic properties of the rare-gas solid Ar at very high pressures up to 70 GPa, which were accomplished by overcoming the problem of Ar recrystallization in the DAC at $P = 4$ GPa. These reliable and wide-range elastic properties provide strong constraints on the best construction of interatomic potentials which are essential for obtaining thermodynamic quantities of the ideal solid Ar at high P-T conditions.

[1] *Rare Gas Solids,* edited by J. A. Venables and M. L. Klein (Academic, New York, 1976), Vols. I and II.
[2] M. I. Eremets *et al.,* Phys. Rev. Lett. **85**, 2797 (2000).
[3] V. F. Lotrich and K. Szalewicz, Phys. Rev. Lett. **79**, 1301 (1997).
[4] K. Rosciszewski *et al.,* Phys. Rev. B **62**, 5482 (2000).
[5] L. W. Finger *et al.,* Appl. Phys. Lett. **39**, 892 (1981).
[6] F. Datchi, P. Loubeyre, and R. LeToullec, Phys. Rev. B **61**, 6535 (2000).
[7] M. Grimsditch, P. Loubeyre, and A. Polian, Phys. Rev. B **33**, 7192 (1986).
[8] H. Shimizu *et al.,* Phys. Rev. Lett. **47**, 128 (1981).
[9] H. Shimizu and S. Sasaki, Science **257**, 514 (1992).
[10] H. Shimizu *et al.,* Phys. Rev. B **53**, 6107 (1996).
[11] S. Gewurtz and B. P. Stoicheff, Phys. Rev. B **10**, 3487 (1974).
[12] H. K. Mao *et al.,* J. Appl. Phys. **49**, 3276 (1978).
[13] P. M. Bell and H. K. Mao, Carnegie Inst. Wash. Yearb. **80**, 404 (1981).
[14] H. Boppart, J. van Straaten, and I. F. Silvera, Phys. Rev. B **32**, 1423 (1985).
[15] G. Zou, P. M. Bell, and H. K. Mao, Carnegie Inst. Wash. Yearb. **81**, 436 (1982).
[16] R. Mock, B. Hillebrands, and R. Sandercock, J. Phys. E **20**, 656 (1987).
[17] M. Ross *et al.,* J. Chem. Phys. **85**, 1028 (1986).
[18] J. S. Tse, V. P. Shpakov, and V. R. Belosludov, Phys. Rev. B **58**, 2365 (1998).
[19] H. Shimizu, T. Kitagawa, and S. Sasaki, Phys. Rev. B **47**, 11 567 (1993).
[20] C. S. Zha *et al.,* Phys. Rev. B **48**, 9246 (1993).
[21] S. Klotz and M. Braden, Phys. Rev. Lett. **85**, 3209 (2000).
[22] M. Born and K. Huang, *Dynamical Theory of Crystal Lattices* (Oxford University, Oxford, 1985), pp. 129–140.
[23] R. A. Aziz and H. H. Chen, J. Chem. Phys. **67**, 5719 (1977).
[24] H. Shimizu, N. Saitoh, and S. Sasaki, Phys. Rev. B **57**, 230 (1998).
[25] V. V. Brazhkin and A. G. Lyapin, Phys. Rev. Lett. **78**, 2493 (1997).
[26] S. V. Sinogeikin and J. D. Bass, Phys. Rev. B **59**, R14 141 (1999).